



PERGAMON

Electrochimica Acta 44 (1998) 853–861

ELECTROCHIMICA  
*Acta*

# The removal of low level organics via hydrogen peroxide formed in a reticulated vitreous carbon cathode cell, Part 1. The electrosynthesis of hydrogen peroxide in aqueous acidic solutions

Alberto Alvarez-Gallegos, Derek Pletcher \*

*The Department of Chemistry, The University, Southampton SO17 1BJ, U.K.*

Received 8 April 1998; received in revised form 22 May 1998

## Abstract

It is demonstrated that hydrogen peroxide can be produced with a current efficiency of 40–70% by the reduction of oxygen at a reticulated vitreous carbon cathode in a divided flow cell using catholytes consisting of aqueous chloride or sulfate media,  $\text{pH} \approx 2$ . The influence of ferrous salts, potential and electrolyte concentration on the current efficiency and rate of  $\text{H}_2\text{O}_2$  production is reported; ferrous ions can lead to the homogeneous decomposition of  $\text{H}_2\text{O}_2$  away from the cathode surface but their effectiveness as a catalyst for this decomposition depends on their speciation in solution which changes during an electrolysis. The conclusions are supported by voltammetry at both a rotating vitreous carbon disc and the reticulated vitreous carbon electrodes. © 1998 Elsevier Science Ltd. All rights reserved.

## 1. Introduction

The past twenty years have seen a revival in interest in the electrosynthesis of hydrogen peroxide by the reduction of oxygen and processes based on both three dimensional cathodes and gas diffusion electrodes have been described [1–5]. Universally, the cathode for this  $2e^-$  reduction of oxygen is carbon. Electrochemical technology for the manufacture of hydrogen peroxide solutions has, however, been limited to high pH where the  $\text{HO}_2^-$  anion has good stability. The same period has seen an extensive effort to develop electrochemical processes for the destruction of organic molecules in effluents and waters [6–8]. One approach for the removal of low concentrations of organics employs the electrogeneration of a chemical oxidising agent to react with the pollutants and systems using chlorine and/or hypochlorite have been available for many years [1, 4].

Hydrogen peroxide is, however, a much more attractive mediator since the reactant can be oxygen from the air and any excess hydrogen peroxide eventually decomposes only to oxygen and water, therefore leaving no residual chemicals in the environment. It is also well known that hydrogen peroxide is a much more powerful oxidant in the presence of a trace of Fe(II) and such additions of Fe(II) would also be acceptable in most environments.

The application of hydrogen peroxide electrogenerated directly in the waste water, however, requires the reduction of oxygen to hydrogen peroxide under quite different conditions from those used in commercial processes for the manufacture of hydrogen peroxide. The medium will generally be close to neutral and may also have a low ionic strength. Indeed, if Fe(II) is to be employed as a catalyst, the medium needs to have  $\text{pH} < 4$  in order for the Fe(II) to remain in solution and a small addition of acid to the wastewater may be essential. It is, however, possible to envisage that both the Fe(II) and  $\text{H}^+$  required could be generated in situ at the anode of an undivided cell generating hydrogen

\* Corresponding author. Tel.: +44-1703-593519; Fax: +44-1703-676960; E-mail: DP1@soton.ac.uk

peroxide at the cathode. Two groups have reported preliminary experiments in H cells with flat plate cathodes which demonstrate that destruction of formaldehyde [9, 10] and phenol [11] via in situ generated hydrogen peroxide is possible and both papers include some data on acidic solutions. A more recent paper [12] describes the efficient destruction of formaldehyde in a flow cell with a reticulated vitreous carbon cathode; it was shown that formaldehyde was oxidised only to formic in alkaline solutions but in slightly acidic media containing Fe(II) oxidation to CO<sub>2</sub> was complete. A Spanish Group have developed the other practical approach based of a gas diffusion cathode and described the complete oxidation of aniline to inorganic products using a slightly acidic solution containing Fe(II) [13–15].

Voltammetric studies of the 2e<sup>-</sup> reduction of oxygen to hydrogen peroxide at carbon cathodes are mainly restricted to high pH solutions where the peroxide is completely stable although Humfray and Taylor [16–18] have reported a study of oxygen reduction at vitreous carbon disc electrodes using both alkaline and acidic solutions.

In this paper, we report a systematic investigation, using both a vitreous carbon rotating disc electrode and a flow cell with a reticulated vitreous carbon cathode of the reduction of oxygen at in slightly acidic solutions with low ionic strengths. Most experiments were carried out with solutions, pH 2, sometimes also with a low concentration of sodium chloride or sulfate. The proton concentration was selected so that oxygen reduction did not produce a significant pH change close to the cathode surface and also so that the solution had sufficient conductivity even in the absence of sodium salt for an acceptable potential/current distribution within the three dimensional cathode.

## 2. Experimental

### 2.1. Chemicals

All solutions were prepared with deionised water (resistivity > 18 MΩ cm) from a MilliQ-MilliRho purification system using hydrogen peroxide (Hogg, 20%), sodium sulfate (BDH, Analar), sulfuric acid (BDH, 98%), sodium chloride (BDH, Analar), hydrochloric acid (Fisons, specific gravity 1.18), ferrous sulfate (Prolabo, 98%), ferrous chloride (Aldrich, 99%), ferric chloride (Fisons, 97%), ferric sulfate (Aldrich, 97%) and potassium permanganate (BDH Analar, 99.5%). All solutions were saturated with either nitrogen or oxygen (both BOC).

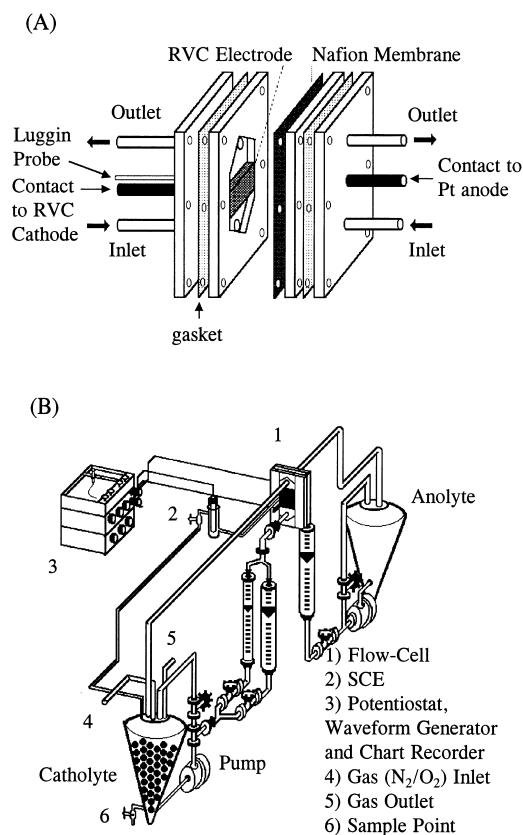


Fig. 1. Sketches of (A) the flow cell with reticulated vitreous carbon cathode and (B) the flow circuit.

### 2.2. Analysis

The hydrogen peroxide was determined by titration with potassium permanganate using a standard procedure [19].

### 2.3. Electrochemical cells and instrumentation

Some voltammetric experiments were carried out in a three electrode, three compartment glass cell with a 4 mm diameter vitreous carbon disc electrode (Pine Instruments), a Pt gauze counter electrode and a laboratory constructed saturated calomel electrode as the reference electrode. All other voltammetry as well as preparative experiments were carried out in a flow cell, see Fig. 1A, with a 50 mm × 50 mm × 12 mm reticulated vitreous carbon (The Electrosynthesis Co., 60 pores per inch) cathode, separated from a Pt gauze anode by a Nafion<sup>®</sup> 450 cation permeable membrane (Aldrich). A plastic tube Luggin capillary entered the three dimensional cathode via a hole drilled through

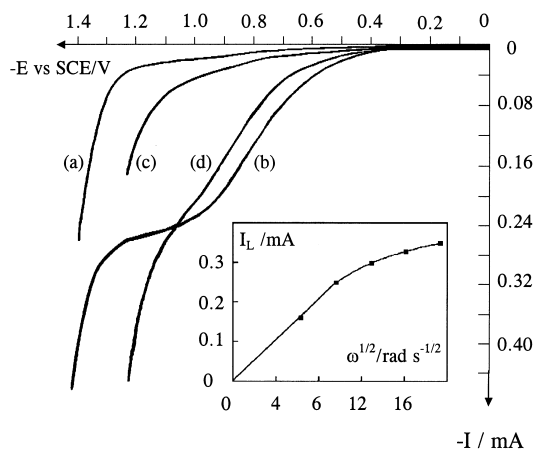


Fig. 2. Voltammograms at a rotating vitreous carbon disc electrode (area  $0.13 \text{ cm}^2$ ). (a) and (b) are for solutions of  $10 \text{ mM HCl} + 100 \text{ mM NaCl}$  saturated with  $\text{N}_2$  and  $\text{O}_2$  respectively. (c) and (d) are for solutions of  $10 \text{ mM HCl}$  saturated with  $\text{N}_2$  and  $\text{O}_2$  respectively. Rotation rate  $900 \text{ rpm}$ . Potential scan rate  $5 \text{ mV s}^{-1}$ . The inset shows the variation of the limiting current for the reduction of  $\text{O}_2$  in  $10 \text{ mM HCl} + 100 \text{ mM NaCl}$  with the rotation rate of the disc.

the cathode current contact. During electrolyte flow through the cell, solution passed through the Luggin probe into the reference electrode compartment; hence, this compartment was fitted with a drain which recycled the electrolyte to the reservoir. The reference electrode was a laboratory constructed saturated calomel electrode (SCE). The anolyte was  $1 \text{ M H}_2\text{SO}_4$  and, in most experiments, the catholyte volume was  $2 \text{ l}$ . This cell and the flow circuit, Fig. 1B, have been fully described in an earlier paper [12].

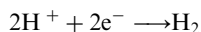
All experiments were carried out at controlled potential using a HiTek potentiostat, model DT2101, and, where appropriate, a HiTek function generator, model PPR1, and a Gould Advance  $x$ - $y$  recorder, model 60000. The rotation of the disc electrode was controlled with an EG and G Parc unit, model 616 and charges were measured on a laboratory constructed digital integrator. Solution pH was determined with a portable M90 pH-meter from Mettler Toledo. The rotating disc voltammetry was carried out at  $298 \text{ K}$  using a jacketed cell and water circulated from a thermostat bath supplied by Grant Instruments, model SE15. Flow cell experiments were carried out in ambient conditions but the temperature settled down to  $300 \pm 2 \text{ K}$  after a few minutes of electrolysis.

### 3. Results and discussion

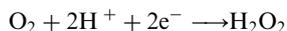
#### 3.1. Voltammetry at a rotating vitreous carbon disc electrode

Relatively little is known about the reduction of oxygen at carbon in aqueous solutions of low acidity and low ionic strength or the influence of iron species on the reaction. Hence a preliminary study was undertaken using a rotating disc electrode.

Fig. 2 shows voltammograms recorded at  $900 \text{ rpm}$  for an aqueous solution of  $10 \text{ mM HCl} + 0.1 \text{ M NaCl}$  saturated with nitrogen and oxygen respectively. In the absence of oxygen, curve (a), little current is observed positive to  $-1200 \text{ mV}$  where  $\text{H}_2$  evolution



can be seen to commence. In the presence of oxygen, curve (b) the voltammogram shows a well formed but rather drawn out reduction wave,  $E_{1/2} = -790 \text{ mV}$  and  $E_{1/4} - E_{3/4} = 220 \text{ mV}$ . In contrast, when  $10 \text{ mM H}_2\text{O}_2$  was added to the deoxygenated solution, the voltammogram was identical to that for the background electrolyte alone; hydrogen peroxide does not reduce on vitreous carbon in this solution at potentials positive to those required for  $\text{H}_2$  evolution. The expected reduction of oxygen at carbon is [11, 16–18]



and this will be confirmed later as the major reaction. The variation of the limiting current for oxygen reduction, measured at  $-1050 \text{ mV}$ , is shown in the inset to Fig. 2. It can be seen that at low rotation rates, the limiting current is proportional to the square root of the rotation rate. Moreover, the measured currents are close to those estimated from the Levich equation (assuming  $n = 2$ ,  $c = 1.3 \text{ mM}$  [20],  $D = 2.2 \times 10^{-5} \text{ cm}^2 \text{ s}^{-1}$ ). At rotation rates above  $900 \text{ rpm}$ , however, the plot of  $I_L$  vs  $\omega^{1/2}$  is non-linear and the reduction of oxygen is only partially mass transfer controlled in these conditions.

Fig. 2 also shows the responses when the voltammograms were repeated in a solution containing only  $10 \text{ mM HCl}$ . In this low ionic strength solution, the reduction currents for oxygen reduction, curve (d), are similar but the wave is less well defined. This is for two reasons. Firstly,  $E_{1/2}$  is shifted more negative by  $\sim 70 \text{ mV}$ . Secondly, and very surprisingly,  $\text{H}_2$  evolution occurs significantly more readily in this solution than in  $10 \text{ mM HCl} + 0.1 \text{ M NaCl}$ . This can also be seen in the voltammogram for the deoxygenated solution, curve (c), where the negative potential limit is shifted positive by  $\sim 130 \text{ mV}$ . The pH of both solutions were measured and found to be  $2.1$  and  $2.0$  for the solution with and without the added NaCl respectively. Hence,

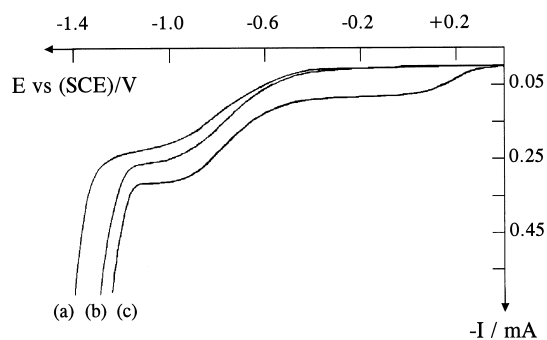


Fig. 3. Voltammograms recorded at a rotating vitreous carbon disc electrode (area  $0.13 \text{ cm}^2$ ) for solutions of  $\text{O}_2$  in 10 mM HCl + 100 mM NaCl containing (a) no added Fe salt (b) 1 mM Fe(II) and (c) 2 mM Fe(III). Rotation rate 900 rpm. Potential scan rate  $5 \text{ mV s}^{-1}$ .

the shift is not associated with a pH difference; nor does it result from uncompensated IR drop. It would appear that the presence of NaCl inhibits the kinetics of  $\text{H}_2$  evolution.

The influence of Fe(II) and Fe(III) on the reduction of oxygen in 10 mM HCl + 100 mM NaCl is reported in Fig. 3 (and voltammograms in sulfate solution are very similar). It can be seen that the addition of either 2 mM Fe(III) or 1 mM Fe(II) has little influence on the reduction wave for oxygen although the presence in solution of an iron species does lead to the catalysis of  $\text{H}_2$  evolution and this results from the deposition of some iron metal on the vitreous carbon surface at potentials more negative than  $-900 \text{ mV}$ . The presence of Fe(III) results, however, in a reduction wave for the process  $\text{Fe}^{3+} \rightarrow \text{Fe}^{2+}$  at  $E_{1/2} = +150 \text{ mV}$ . Although the concentrations of Fe(III) and  $\text{O}_2$  are similar (2 and 1.3 mM [20], respectively), the mass transfer controlled limiting currents are quite different because of different diffusion coefficients ( $0.5 \times 10^{-5}$  and  $2.2 \times 10^{-5} \text{ cm}^2 \text{ s}^{-1}$ , respectively). The experiments also showed that the reaction of oxygen with Fe(II) is very slow in these solutions –the voltammogram for the solution containing Fe(II) +  $\text{O}_2$  did not change over several hours.

When the experiments were repeated in sulfate media, the voltammograms were very similar to those reported above for chloride media.

### 3.2. Voltammetry at a reticulated vitreous carbon cathode in a flow cell

The voltammetry was repeated in the cell with a 60 ppi reticulated vitreous carbon cathode ( $50 \text{ mm} \times 50 \text{ mm} \times 12 \text{ mm}$ ) and a mean linear catholyte flow rate of  $0.13 \text{ m s}^{-1}$ . Typical voltammograms in 10 mM HCl are reported in Fig. 4. The oxygen saturated solution gives a rather featureless response without a clear reduction wave, curve (a). On the other hand, over a

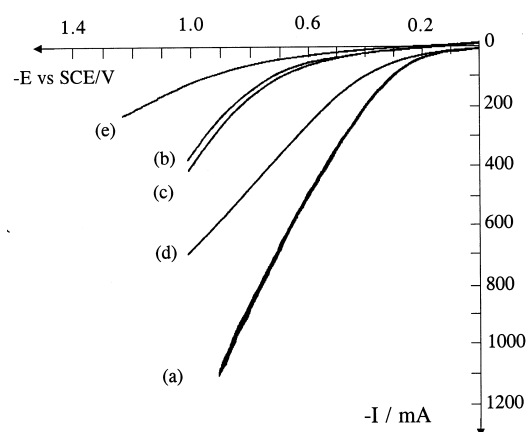


Fig. 4. Voltammograms recorded at a  $50 \text{ mm} \times 50 \text{ mm} \times 12 \text{ mm}$  reticulated vitreous carbon electrode (60 ppi) in solutions of (a)  $\text{O}_2$  saturated 10 mM HCl (b)  $\text{N}_2$  saturated 10 mM HCl (c) 6 mM  $\text{H}_2\text{O}_2$  in 10 mM HCl (d)  $\text{O}_2$  saturated 10 mM HCl + 500 mM NaCl (e)  $\text{N}_2$  saturated 10 mM HCl + 500 mM NaCl. Catholyte flow rate  $0.13 \text{ m s}^{-1}$ . Potential scan rate  $5 \text{ mV s}^{-1}$ .

wide potential range negative to  $-200 \text{ mV}$ , the current is much higher than for the deoxygenated solution, curve (b). Indeed, the current increases smoothly with potential and reaches a value  $\sim 1.1 \text{ A}$  ( $37 \text{ mA cm}^{-3}$ ) at  $-900 \text{ mV}$ . This compares with the expected mass transfer limited current of  $115 \text{ mA cm}^{-3}$  for a 1.3 mM solution of  $\text{O}_2$  calculated using  $n = 2$  and a value of  $k_{\text{m}}A_{\text{e}} = 0.44 \text{ s}^{-1}$ , estimated using a value from [21] and allowing for the large diffusion coefficient for  $\text{O}_2$ . The degree to which the response is distorted by IR drop is unknown but it is certainly clear that the use of the three dimensional electrode permits the reduction of oxygen at a high rate. It should also be noted that the cathodic current for oxygen reduction is observed over the same potential range as at the rotating vitreous carbon disc electrode.

Fig. 4 reports two further results. Curve (c) for 6 mM  $\text{H}_2\text{O}_2$  in 10 mM HCl shows that hydrogen peroxide does not reduce on reticulated vitreous carbon, at least positive to  $-1000 \text{ mV}$  where  $\text{H}_2$  evolution commences. Curves (d) and (e) illustrate the effect of recording voltammograms for solutions with a large excess of sodium chloride. It can be seen that the addition of 0.5 M NaCl (which changes the pH from 2.1 to 1.7) decreases substantially the current for  $\text{H}_2$  evolution. This change in the voltammograms is the same as observed with the rotating vitreous carbon disc electrode but it is contrary to that predicted from considerations of pH or uncompensated IR drop or structure of the double layer. The voltammogram for the oxygen saturated solution also shows less current (e.g. 0.7 A cf 1.1 A at  $-900 \text{ mV}$ ) after the addition of the 0.5 M NaCl. This results partly from a decrease in

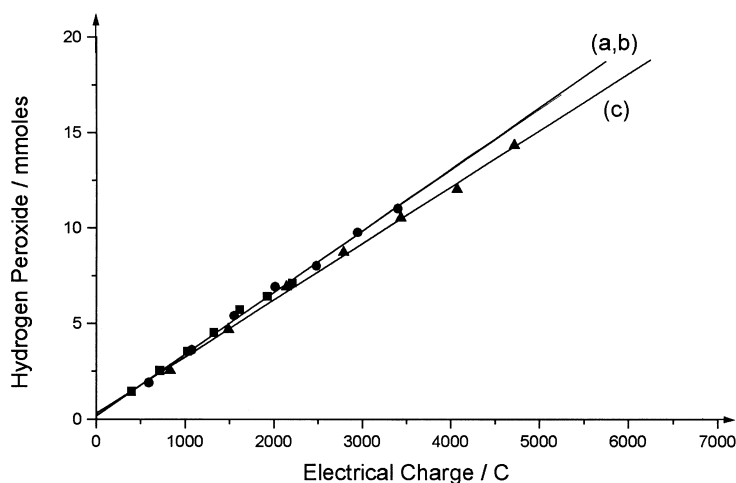


Fig. 5. Plots of hydrogen peroxide formation in the catholyte versus charge passed during electrolyses of 10 mM HCl + 50 mM NaCl continuously saturated with oxygen. The electrolyses were carried out at constant potentials of (a)  $-500$  mV, (b)  $-600$  and  $-700$  mV vs SCE. Catholyte flow rate  $0.13 \text{ m s}^{-1}$ .

the  $\text{H}_2$  evolution current and partly from the decreased solubility of  $\text{O}_2$  in the higher ionic strength medium.

The addition of 1 mM Fe(II) to either electrolyte medium did not change the voltammograms for the reduction of oxygen. Moreover, the responses in sulfate media were essentially identical to those shown above for chloride solutions.

### 3.3. Electrolyses in the absence of Fe(II)

Electrolyses were carried out in the flow cell with a reticulated vitreous carbon electrode and a cation permeable membrane. In all experiments, the catholyte was continuously saturated with oxygen by bubbling the gas through the reservoir and the hydrogen peroxide concentration was monitored periodically by titrating samples with potassium permanganate. Fig. 5 reports the build up of hydrogen peroxide with time

within the catholyte for three electrolyses carried out in 10 mM HCl + 50 mM NaCl at different potentials. It can be seen that the concentration of hydrogen peroxide increases linearly with time and the slopes of the plots are not a strong function of potential. In all three electrolyses, the current efficiency is  $60 \pm 3\%$  for the formation of hydrogen peroxide. Moreover in longer timescale electrolyses, the concentration of hydrogen peroxide could be taken to  $> 20$  mM.

Table 1 and 2 report data from more extensive set of experiments, carried out as a function of potential and ionic strength in both chloride and sulfate solutions of pH close to 2. Over an extended range of conditions, the current efficiency fell within the range 50–70% and electrolyte flow rate also has no significant effect. At the most negative potentials, the current efficiency dropped due to competing  $\text{H}_2$  evolution. As expected from the voltammetry, this was most marked

Table 1. Cell currents,  $I$ , current efficiencies,  $\phi$  and rates of  $\text{H}_2\text{O}_2$  generation,  $R$ , in chloride solutions as a function of electrode potential and ionic strength

$-E/V$ vs SCE	10 mM HCl + 50 mM NaCl			10 mM HCl + 100 mM NaCl			10 mM HCl + 500 mM NaCl					
	$-I/A$	$\phi$ (%)	$R$ ( $\mu\text{moles s}^{-1}$ )	$-I/A$	$\phi$ (%)	$R$ ( $\mu\text{moles s}^{-1}$ )	$-I/A$	$\phi$ (%)	$R$ ( $\mu\text{moles s}^{-1}$ )	$-I/A$	$\phi$ (%)	$R$ ( $\mu\text{moles s}^{-1}$ )
400	0.17	57	0.54	0.15	61	0.46	0.12	43	0.26	0.12	39	0.24
500	0.32	56	0.90	0.25	61	0.76	0.26	62	0.81	0.27	54	0.86
600	0.44	48	1.06	0.39	62	1.21	0.35	63	1.10	0.33	51	0.84
700	0.61	41	1.25	0.55	57	1.57	0.44	63	1.39	0.42	58	1.22
800	0.82	16	0.66	0.64	49	1.57	0.57	56	1.62	0.57	58	1.65
900				0.85	39	1.66	0.73	48	1.75	0.60	58	1.74

Flow cell with 60 ppi reticulated vitreous carbon cathode. Mean linear catholyte flow rate  $0.13 \text{ m s}^{-1}$ . Temperature 300 K.

Table 2. Cell currents,  $I$ , current efficiencies,  $\phi$  and rates of  $\text{H}_2\text{O}_2$  generation,  $R$ , in sulfate solutions (columns 1–4) for 10 mM  $\text{H}_2\text{SO}_4$  + 50 mM  $\text{Na}_2\text{SO}_4$  as a function of electrode potential and (columns 5–8) at  $-500$  mV vs SCE as a function of sodium sulfate concentration added to 10 mM  $\text{H}_2\text{SO}_4$

$-E/V$ vs SCE	$-I/A$	$\phi$ (%)	$R$ ( $\mu\text{moles s}^{-1}$ )	$[\text{Na}_2\text{SO}_4]$ (mM)	$-I/A$	$\phi$ (%)	$R$ ( $\mu\text{moles s}^{-1}$ )
400	0.13	62	0.40	0	0.30	50	0.75
500	0.26	68	0.88	50	0.26	68	0.88
600	0.29	61	0.94	100	0.26	62	0.81
700	0.43	63	1.35	500	0.23	69	0.79
800	0.55	52	1.43				
900	0.77	36	1.39				

Flow cell with 60 ppi reticulated vitreous carbon cathode. Mean linear catholyte flow rate  $0.13 \text{ m s}^{-1}$ . Temperature 300 K.

in solutions without the addition of a sodium salt to increase the ionic strength. Clearly, the current efficiencies are always significantly below 100% and this is in contrast to electrolyses in NaOH solutions where the current efficiencies were generally  $>90\%$  [12, 21]. Hydrogen peroxide was found to be stable over many hours in these pH 2 solutions even when flowing through the cell on open circuit and hence the lower current efficiencies cannot be attributed to homogeneous chemical decomposition. Moreover,  $\text{H}_2\text{O}_2$  does not reduce at the vitreous carbon cathode, see the voltammogram shown as Fig. 4(c). Therefore, it must be concluded that at these vitreous carbon surfaces, oxygen reduction occurs by a mechanism where there is competition between a  $2e^-$  pathway and a  $4e^-$  pathway without  $\text{H}_2\text{O}_2$  as a discrete intermediate; similar conclusions have been drawn by other authors [11, 16–18]. The ratio of the two pathways is independent of the potential and it is likely that they correspond to reduction at two different types of site on the carbon surface. The tables also reports the average cell currents during the electrolyses, which, of course increase as the potential is made more negative as well as the rates of production of  $\text{H}_2\text{O}_2$  in  $\mu\text{moles s}^{-1}$  since in effluent treatment applications this may be more important than the current efficiency when values are so similar over a range of conditions. With the exception of one solution, the highest rate of  $\text{H}_2\text{O}_2$  production always occurs at  $-900$  mV; the increase in current is more important than the loss in current efficiency.

It should also be stressed that no bulk pH change was observed during the electrolysis; this is to be expected since  $1\text{H}^+/1e^-$  passes through the membrane and  $1\text{H}^+/1e^-$  is consumed at the cathode. The local increase in pH at the cathode surface will also be small since  $c_{\text{H}^+} > c_{\text{O}_2}$ .

### 3.4. Electrolyses in the presence of Fe(II)

When the electrolyses were repeated with 1 mM Fe(II) added to the catholytes studied, it was found

that the current efficiency for the production of hydrogen peroxide was negligible over an extended period of time. It was also found that the addition of 1 mM Fe(II) to solutions of hydrogen peroxide in either chloride or sulfate media, pH  $\approx 2$ , led to the homogeneous decomposition over a period of a few minutes.

On the other hand, it was reported in Sections 3.1 and 3.2, that the addition of Fe(II) to the solutions had little influence on the voltammetry. If the Fe(II) catalysed disproportionation of hydrogen peroxide were rapid, one would expect to a change from  $2e^-$  waves to  $4e^-$  reduction waves, reflecting the regeneration of oxygen with the boundary layer at the electrode surface. Moreover, conclusive evidence for the formation of hydrogen peroxide throughout the electrolyses in the presence of Fe(II) results from studies of the in situ oxidation of organic pollutants during the reduction of oxygen [22]; a number of organic pollutants are oxidised with good efficiency. Hence, it must be concluded that hydrogen peroxide is, indeed, formed at the reticulated vitreous carbon cathode even in the presence of Fe(II) but it decomposes in solution in a reaction which is slow enough that it occurs away from the cathode surface.

It was also found during extended electrolyses that eventually the hydrogen peroxide concentration in the catholyte began to rise. Fig. 6A shows a plot of hydrogen peroxide concentration versus time for an electrolysis carried out at  $-700$  mV vs SCE and a catholyte consisting of 50 mM  $\text{Na}_2\text{SO}_4$  + 1 mM Fe(II), adjusted to pH 1.6 with  $\text{H}_2\text{SO}_4$ , with data from a similar experiment without Fe(II) for comparison. The cell current remained at 0.4 A throughout both electrolyses. In the presence of Fe(II), the current efficiency for hydrogen peroxide is close to 0% during the passage the first 4000 C of charge ( $\sim 100$  min). Thereafter, the current efficiency begins to improve and by 12000 C, it is  $\sim 30\%$ . The figure also shows that the addition of a further aliquot of Fe(II) equivalent to 1 mM after 500 min leads to the rapid destruction of all the hydrogen peroxide in the catholyte as well as preventing the accumulation of further hydrogen peroxide for another

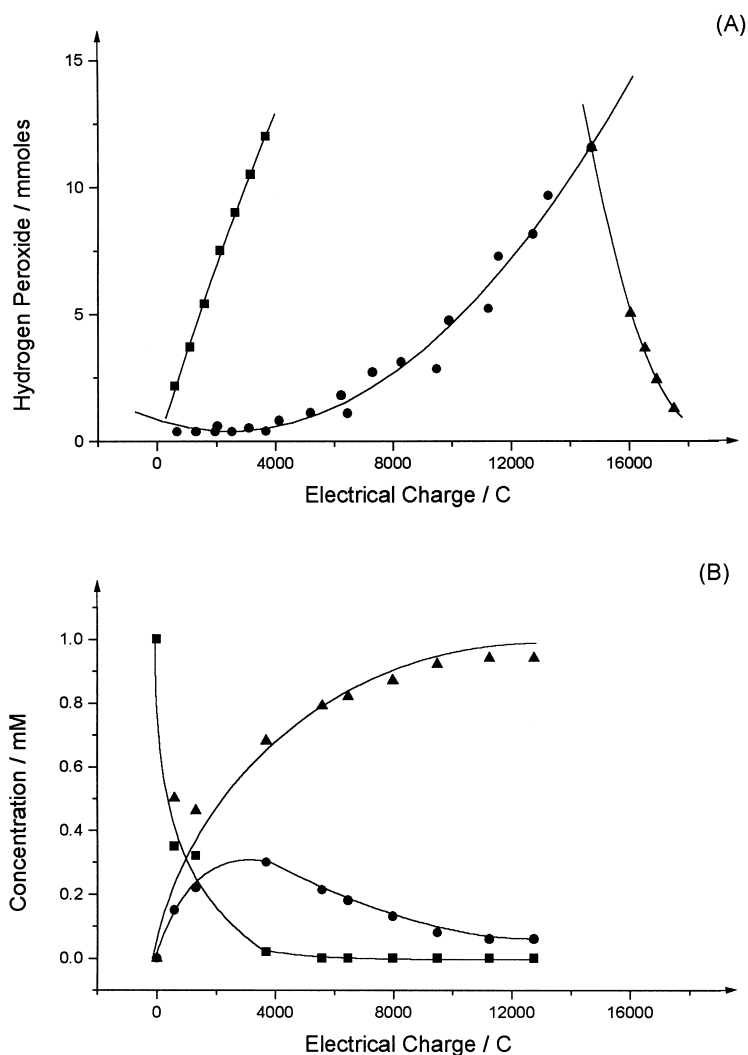


Fig. 6. Electrolyses at  $-700$  mV vs SCE of 50 mM Na<sub>2</sub>SO<sub>4</sub> adjusted to pH 1.6 continuously saturated with O<sub>2</sub> at a reticulated vitreous carbon cathode in a flow cell. (A) Plots of H<sub>2</sub>O<sub>2</sub> formed versus charge passed for solutions with ■ 0 mM added Fe(II) ● 1 mM added Fe(II) ▲ further 1 mM Fe(II) added. (B) concentrations of ■ Fe(II) ● Fe(III) ▲ added Fe no longer present as soluble, electroactive species as a function of charge passed.

extended period. During the electrolysis, aliquots of the catholyte were taken and voltammograms were recorded for each at a rotating vitreous carbon disc electrode between the potential limits, +1100 and  $-400$  mV vs SCE. The oxidation and reduction waves observed at  $E_{1/2} = +780$  and  $+15$  mV were used to estimate the concentrations of Fe(II) and Fe(III) respectively in the catholyte as a function of time during the electrolysis. The results are shown in the inset to Fig. 6B. It can be seen that the concentration of Fe(II) decays steadily and has dropped to zero after about 4000 C. In contrast, the concentration of Fe(III) increases over this period of electrolysis and then

passes through a broad maximum until it is almost zero after 13000 C. It is clear, however, that the total concentration of electroactive Fe species in the catholyte drops throughout the electrolysis and these data are also shown in Fig. 6B. The addition of a further 1 mM Fe(II) to the catholyte after 13000 C leads to the instant conversion of most of this Fe(II) to Fe(III). The total loss of Fe(II) from the catholyte coincides with the formation of some stable hydrogen peroxide and it would appear that the Fe(II) is a much more efficient catalyst than the Fe(III) for the decomposition of hydrogen peroxide.

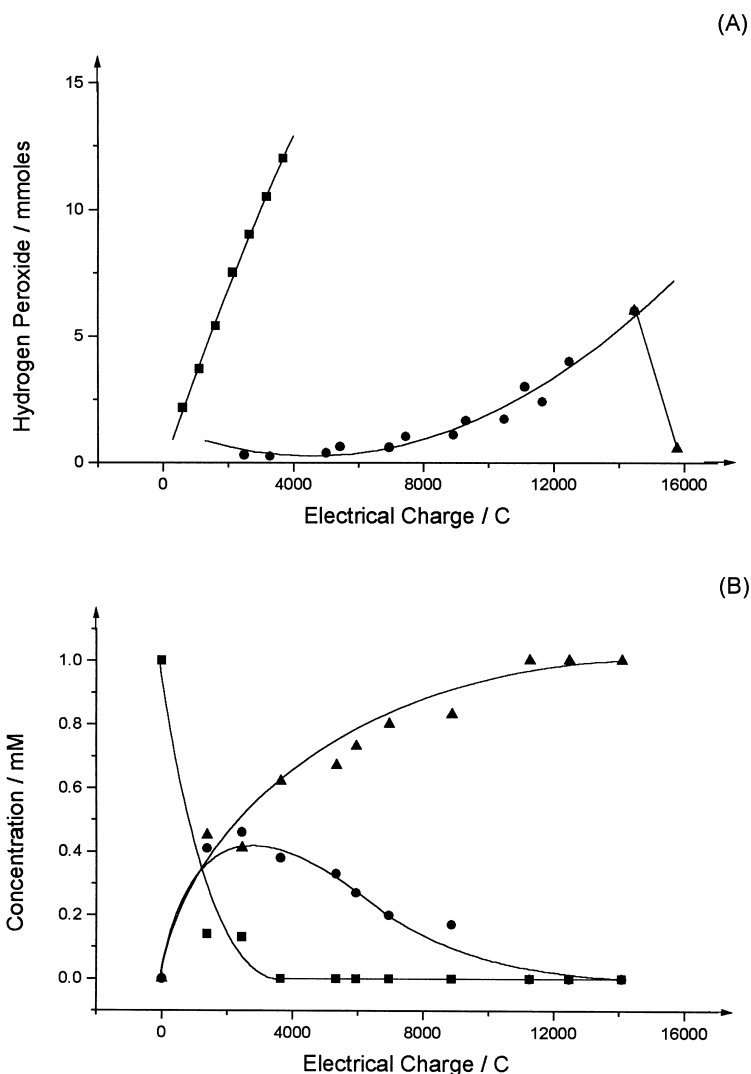


Fig. 7. Electrolyses at  $-700$  mV vs SCE of  $10$  mM HCl +  $10$  mM NaCl continuously saturated with  $O_2$  at a reticulated vitreous carbon cathode in a flow cell. (A) Plots of  $H_2O_2$  formed versus charge passed for solutions with  $\blacksquare$   $0$  mM added Fe(II)  $\bullet$   $1$  mM added Fe(II)  $\blacktriangle$  further  $1$  mM Fe(II) added. (B) concentrations of  $\blacksquare$  Fe(II)  $\bullet$  Fe(III)  $\blacktriangle$  added Fe no longer present as soluble, electroactive species as a function of charge passed.

Fig. 7 reports the results from an identical experiment using a catholyte consisting of  $10$  mM NaCl +  $10$  mM HCl both with and without the addition of  $1$  mM Fe(II). Although the current efficiency for hydrogen peroxide production is always lower than in the sulfate medium, the variation of hydrogen peroxide concentration with charge passed is similar to that in sulfate medium. Fig. 7B shows the charge evolution of Fe(II) and Fe(III) concentrations in the chloride medium and this also follows the trends noted above for the sulfate solution.

Therefore, in both media it is apparent that the Fe(II) is converted to Fe(III) by reaction either with

oxygen and/or hydrogen peroxide and this results in a loss of catalytic activity for the decomposition of hydrogen peroxide. Thereafter, the Fe(III) is also converted to an electroinactive form. Most likely the Fe(III) precipitates as a ferric oxide/hydroxide solid or colloid or adsorbs on a surface within the flow system although a precipitate cannot be seen in the catholyte.

#### 4. Conclusions

The voltammetry and preparative electrolyses both confirm that hydrogen peroxide may be formed by

cathodic reduction of oxygen at vitreous carbon in slightly acidic, aqueous solutions. The hydrogen peroxide may be prepared in 10 mM acid without other electrolytes and although the addition of electrolyte does improve the current efficiency to some extent, it does not increase the rate of production. The current efficiency at  $\text{pH} \approx 2$  is, however, always significantly below 100% and the current efficiency is not a strong function of either potential or the catholyte composition; this is consistent with  $2e^-$  and  $4e^-$  reductions of oxygen occurring in parallel at different sites on the carbon surface.

The presence of Fe(II) in the catholyte does not prevent the formation of hydrogen peroxide at the cathode but can catalyse the homogeneous decomposition and in the presence of 1 mM Fe(II) the half life of the hydrogen peroxide is minutes. The ability of the iron species in solution to catalyse hydrogen peroxide decomposition is, however, very dependent on its form which changes during the electrolysis; while freshly added Fe(II) is an efficient catalyst for hydrogen peroxide decomposition, its effectiveness decreases with electrolysis time.

Certainly, the use of a three dimensional electrode fabricated from reticulated vitreous carbon allows hydrogen peroxide to be produced at  $\text{pH} \approx 2$  at a rate which makes possible, for example, the use of this approach for effluent treatment [22].

#### Acknowledgements

The authors would like to thank the Consejo Nacional de Ciencia y Tecnología de México for support of the work through a grant to A. A.-G.

#### References

- [1] D. Pletcher, F.C. Walsh, 1990. *Industrial Electrochemistry*. Chapman and Hall, London.
- [2] J.A. McIntyre, *Interface* 4 (1995) 29.
- [3] F.C. Foller, R.T. Bombard, *J. Appl. Electrochem.* 25 (1995) 613.
- [4] P. Tatapudi, J.N. Fenton, 1994. In: Sequeira, C.A.C. (Ed.), *Environmental Orientated Electrochemistry*. Elsevier, Amsterdam.
- [5] C. Oloman, 1996. *Electrochemical Processing for the Pulp and Paper Industry*. The Electrochemical Consultancy, Romsey, UK.
- [6] J.D. Genders, N.L. Weinberg, (Eds.), 1992. *Electrochemistry for a Cleaner Environment*. The Electrosynthesis, Lancaster, New York.
- [7] K. Rajeshwar, J. Ibanez, 1997. *Environmental Electrochemistry: Fundamentals and Applications in Pollution Abatement*. Academic Press, San Diego.
- [8] C. Comninellis, 1994. In: Sequeira, C.A.C. (Ed.), *Environmental Orientated Electrochemistry*. Elsevier, Amsterdam.
- [9] J.-S. Do, C.-P. Chen, *J. Electrochem. Soc.* 140 (1993) 1632.
- [10] J.-S. Do, C.-P. Chen, *J. Appl. Electrochem.* 24 (1994) 936.
- [11] M. Sudoh, T. Kodera, K. Sakai, J.Q. Zhang, K. Koide, *J. Chem. Eng. Jpn.* 19 (1986) 513.
- [12] C. Ponce de Leon, D. Pletcher, *J. Appl. Electrochem.* 25 (1995) 307.
- [13] E. Brillas, R.M. Bastida, E. Llosa, J. Casado, *J. Electrochem. Soc.* 142 (1995) 1733.
- [14] E. Brillas, E. Mur, J. Casado, *J. Electrochem. Soc.* 143 (1996) L49.
- [15] E. Brillas, R. Sauleda, J. Casado, *J. Electrochem. Soc.* 144 (1997) 2374.
- [16] R.J. Taylor, A.A. Humffray, *J. Electroanal. Chem.* 64 (1975) 63.
- [17] R.J. Taylor, A.A. Humffray, *J. Electroanal. Chem.* 64 (1975) 85.
- [18] R.J. Taylor, A.A. Humffray, *J. Electroanal. Chem.* 64 (1975) 95.
- [19] I.M. Kolthoff, R. Belcher, 1957. *Volumetric Analysis*, vol. 3. *Titration Methods: Oxidation Reduction Reactions*. Interscience, New York.
- [20] E.W. Washburn, (Ed.), 1928. *International Critical Tables of Numerical Data in Physics, Chemistry and Technology*, vol. III. McGraw-Hill, p. 272.
- [21] D. Pletcher, I. Whyte, F.C. Walsh, J.P. Millington, *J. Appl. Electrochem.* 21 (1991) 659.
- [22] D. Pletcher, A. Alvarez-Gallegos, in preparation.